Monitoring attosecond dynamics of coherent electron-nuclear wave packets by molecular high-order-harmonic generation

Timm Bredtmann,[1,2] Szczepan Chelkowski,[1] and André D. Bandrauk[1]

[1]*Laboratoire de Chimie Théorique, Faculté des Sciences, Université de Sherbrooke, Sherbrooke, Québec, Canada J1K 2R1*
[2]*Institut für Chemie und Biochemie, Freie Universität Berlin, Takustrasse 3, D-14195 Berlin, Germany*

A pump-probe scheme for preparing and monitoring electron-nuclear motion in a dissociative coherent electron-nuclear wave packet is explored from numerical solutions of a non-Born-Oppenheimer time-dependent Schrödinger equation. A mid-ir intense few-cycle probe pulse is used to generate molecular high-order-harmonic generation (MHOHG) from a coherent superposition of two or more dissociative coherent electronic-nuclear wave packets, prepared by a femtosecond uv pump pulse. Varying the time delay between the intense ir probe pulse and the uv pump pulse by a few hundreds of attoseconds, the MHOHG signal intensity is shown to vary by orders of magnitude, thus showing the high sensitivity to electron-nuclear dynamics in coherent electron-nuclear wave packets. We relate this high sensitivity of MHOHG spectra to opposing electron velocities (fluxes) in the electron wave packets of the recombining (recolliding) ionized electron and of the bound electron in the initial coherent superposition of two electronic states.

PACS number(s): 33.80.Wz, 42.50.Hz

Ultrashort laser pulses allow for the imaging of microscopic molecular structures and thus reconstructing both electron and nuclear motion [1]. Recently, pulses as short as 80 as have been obtained allowing one, in principle, to monitor electron motion in matter [2,3], in particular in coherent superpositions of atomic or molecular orbitals, which result in nonstationary time-dependent electronic states [4,5]. Molecules add other variables to monitor electron dynamics on femtosecond - attosecond time scales due to the femtosecond time scale for nuclear motion such as in the H_2 molecule, whose vibrational period of 7 fs was shown earlier to significantly control molecular high-order-harmonic generation (MHOHG) [6], where the 2/3 cycle time of a recombining ionized electron as predicted by the simple three-step recollision model [1–3,7] becomes comparable to the vibrational periods t_ν of H_2^+ ($t_\nu \approx 10$ fs) and of H_2 ($t_\nu \approx 7$ fs). Monitoring electron motion in coherent electron-nuclear wave packets (CEWPs) created by ultrashort pulses was investigated earlier at fixed internuclear distance from Born-Oppenheimer solutions of the time-dependent Schrödinger equation (TDSE) for H_2^+ [4,5]. The temporal asymmetry of an attosecond photoionization spectrum was shown to be a faithful measure of electron motion with an attosecond time scale in a CEWP comprising a combination of $\sigma_g 1s$ and $\sigma_u 1s$ molecular orbitals, thus monitoring electron transfer between both stationary protons. Including nuclear motion in a subsequent non-Born Oppenheimer simulation of the same system showed that a coherent dissociative electron-nuclear wave packet formed from coherent excitation on an attosecond time scale of both $\sigma_g 1s$ and $\sigma_u 1s$ electron-proton states reproduced a similar attosecond time-dependent asymmetric photoionization spectrum indicative of electron transfer on an attosecond time scale [8]. This asymmetry disappeared after a few-femtosecond time delay between the pump pulse creating the CEWP and the attosecond probe photoionization pulse. This was shown to be the result of vanishing overlap between the rapidly dissociating excited state ($\sigma_u 1s$) nuclear wave packet and the initial $\nu = 0$ vibrational ground-state ($\sigma_g 1s$) localized

nuclear wave function. The disappearence of asymmetric photoionization was shown to be delayed in the molecular ion T_2^+ due to slower moving nuclei [8]. Such suppression of oscillatory physical phenomenon due to coherent quantum state superposition is generally attributed to *decoherence* [9]. For the CEWP reported in Ref. [8] the suppression of coherent electron motion, corresponding to electron transfer, measured by the oscillatory asymmetry in attosecond photoionization, was clearly related to ultrafast femtosecond nuclear (proton) motion on the dissociative excited $\sigma_u 1s$ potential. High-order harmonic generation (HOHG) from a coherent superposition of two electronic states has been described in the strong-field approximation (SFA) theoretically for atoms [10] as well as the corresponding MHOHG spectra for the Born-Oppenheimer H_2^+ system [11] and the $H^+ + H_2^+$ system at various fixed internuclear distances [12]. In these studies, the dependence of the spectra on the time delay between the pump pulse preparing the CEWP and the probe pulse for MHOHG was not explicitly investigated theoretically. A recent experimental MHOHG study from a molecular CEWP in the dissociating Br_2 molecule was reported in Ref. [13], where it was shown that at large internuclear distance where there is no longer nuclear overlap between the initial bound and dissociative excited state, similar to H_2^+ [8], the harmonics generated by the electronically excited state still interfere with harmonics generated by the ground state. In the present work we solve numerically a one-dimensional TDSE describing the dynamics of a T_2^+ molecular ion driven by a weak uv pump pulse and an intense 800-nm probe pulse. We have chosen a T_2^+ molecule since in H_2^+ the dissociation is so fast that already during the preparation of a combined electron-nuclear wave packet using a few-femtosecond uv pump pulse the nuclear wave packet loses considerably its overlap with the initial bound vibrational state as shown in Ref. [8]. In Ref. [14] it was shown that signals of ionization induced by attosecond electron pulses are more clear in T_2^+ than in H_2^+. Moreover, since as a probe we are not using an attosecond pulse but a much longer pulse than in Ref. [8] a heavier molecule than
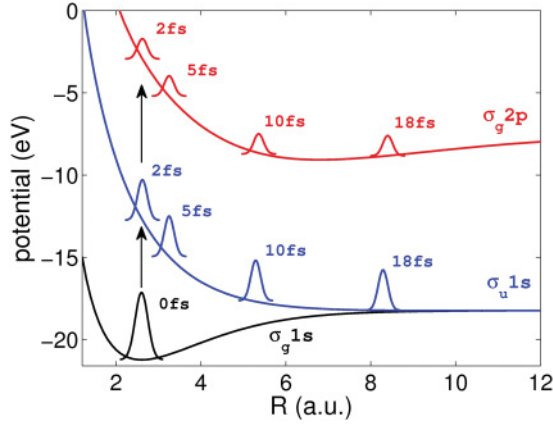
FIG. 1. (Color online) Illustration of the nuclear wave packet dynamics in the T_2^+ molecular ion following excitation by a femtosecond uv pump pulse.

H_2^+ must be used. For each fixed time delay t_{del} between the pump and probe we have solved numerically the complete, three-body, one-dimensional (1D) TDSE for a T_2^+ molecule (atomic units, a.u., $e = \hbar = m_{el} = 1$ are used):

$$i \frac{\partial \psi(z,R,t)}{\partial t} = H(z,R,t)\psi(z,R,t), \quad (1)$$

including both electronic and nuclear degrees of freedom, where $H(z,R,t)$ is the *exact* three-body Hamiltonian in 1D, z is the electron coordinate (with respect to the nuclear center of mass), and R is the internuclear distance (see Ref. [8] for details). The electric field we use is the sum of the field of the pump uv laser pulse which prepares the dissociating wave packet and an 800-nm fewfemtosecond intense probe pulse which generates the harmonics, $E(t) = E_{pump}(t) + E_{probe}(t)$. The electric field for each pulse is defined via the vector potential $A(t)$ [15]. Sine-squared functions are used for the envelopes of the A field of each pulse as in Refs. [8,15]. The time delay between pump and probe pulse is defined as the time difference between the maxima of the respective pulse envelopes. The carrier envelope phase (CEP) φ of both pulses (as defined in Ref. [15]) is equal to $\pi/2$, i.e., a sine pulse is used. The total durations of the pump and probe pulses are 2.7 fs [1 fs full width at half maximum (FWHM)] and 5.3 fs (1.94 fs FWHM), respectively.

We have obtained numerically the time evolution of the total electron-nuclear wave function $\psi(z,R,t)$ using the second-order accurate split-operator method [8]. Next, we calculate the electron acceleration $a(t) = -E(t) - \langle \psi | \frac{\partial V_C}{\partial z} | \psi \rangle$, where $V_C(z,R)$ is the potential describing the Coulomb attraction from the two nuclei [8,12] and its Fourier transform $F(\omega, t_{del})$ (we integrate over time until $t_e = t_{end} + 7.3$ fs, where t_{end} is the end of the probe pulse). The power spectrum of the generated harmonics, plotted in Fig. 2, is equal to $|F(\omega, t_{del})|^2$ [12]. We suppose that initially, at $t = 0$, the T_2^+ molecule is in its ground vibrational state ($\nu = 0$) on the $\sigma_g 1s$ bound potential. The pump laser pulse which prepares the coherent superposition of the two lowest electronic surfaces, $\sigma_g 1s$ (bound) and $\sigma_u 1s$ (dissociative), see Fig. 1, has the angular frequency ω_{pump} which is equal to the energy difference between these surfaces, i.e., is resonant with the transition from the $\sigma_g 1s$ to the $\sigma_u 1s$

TABLE I. Laser parameters and populations for schemes I–III. Frequencies are in a.u. and laser intensities are in W/cm^2.

Scheme	ω_{pump}	I_{pump}	I_{probe}	$\sigma_u 1s$	$\sigma_g 2p$
I	0.33	10^{13}	2×10^{14}	0.16	0.03
II	0.33	10^{12}	4×10^{14}	0.02	4×10^{-4}
III	0.28	10^{11}	4×10^{14}	3×10^{-3}	3×10^{-6}

surface. This scheme prepares a dissociating wave packet on the repulsive surface $\sigma_u 1s$. However, as seen in Fig. 1, it can also prepare a wave packet on the higher electronic surface $\sigma_g 2p$ via a two-photon resonance. Figure 1 shows a sketch of the nuclear wave packets (prepared by the pump pulse alone) on all three surfaces, for various times for scheme I (Table I).

For this first scenario, scheme I, we have chosen a relatively intense pump pulse, $I_{pump} = 10^{13}$ W/cm^2, which prepares a considerable population on the two dissociative $\sigma_u 1s$ and $\sigma_g 2p$ states, and a relatively weak probe intensity $I_{probe} = 2 \times 10^{14}$ W/cm^2. We plot as a contour graph in Fig. 2(a) the harmonic spectrum as function of the time delay t_{del} between pump and probe and in Fig. 2(b) the signal from the 27th- and 35th-order harmonic. We observe very sharp, up to 4 orders of magnitude, changes in the harmonic signal showing a periodicity of 400 as corresponding to $\tau_{1,2} = 2\pi/(E_2 - E_1) \simeq 2\pi/(E_3 - E_2) = \tau_{2,3}$, where E_j, $j = 1,2,3$, are the electronic energies. The spacings between the two upper states depend little on the nuclear distance (Fig. 1), thus leading to a steady oscillatory period $\tau_{2,3}$ up to large pump-probe delays t_{del}. We see in Fig. 1 that we generate nuclear wave packets on both upper surfaces which continue overlapping over large internuclear distances, whereas both lose their overlap with the ground state about 5 fs after the start of the uv pump pulse. As a result we do not see any decay of the oscillation amplitude in scheme I (Fig. 2). Note that at $R = 2.6$ a.u. (equilibrium separation in our 1D model) the ionization potential from the ground $\sigma_g 1s$ state is rather high ($I_p = 31.7$ eV). We have checked that the overall harmonic signal from the ground state $\sigma_g 1s$ is over 7 orders of magnitude weaker than the harmonic generation from the upper dissociative states. Consequently, in scheme I we do not expect any contribution to harmonics from the ground state. Thus we conclude that in the case of scheme I we see the steady effect of coherence, via oscillations of period 400 as from only the two upper states. This conclusion is supported by the harmonics seen in the case of schemes II and III. In scheme II we increase the contribution from the ground state E_1 by increasing the probe intensity to $I_{probe} = 4 \times 10^{14}$ W/cm^2 and decreasing the populations in the upper states E_2 and E_3 by lowering the pump intensity to $I_{probe} = 10^{12}$ W/cm^2. We clearly see in Figs. 2(a) and 2(b), scheme II, the oscillations due to the coherence between the two lower states for delays t_{del} smaller than 3 fs and their decay at larger delays due to the loss of the overlap between the nuclear wave packets, as seen in Fig. 1. However, at larger time delay the amplitude of oscillation increases again and becomes similar to that in scheme I, showing the signature of coherence between the two upper surfaces. In order to get rid entirely of the contribution of the highest $\sigma_g 2p$ state, we decrease in scheme
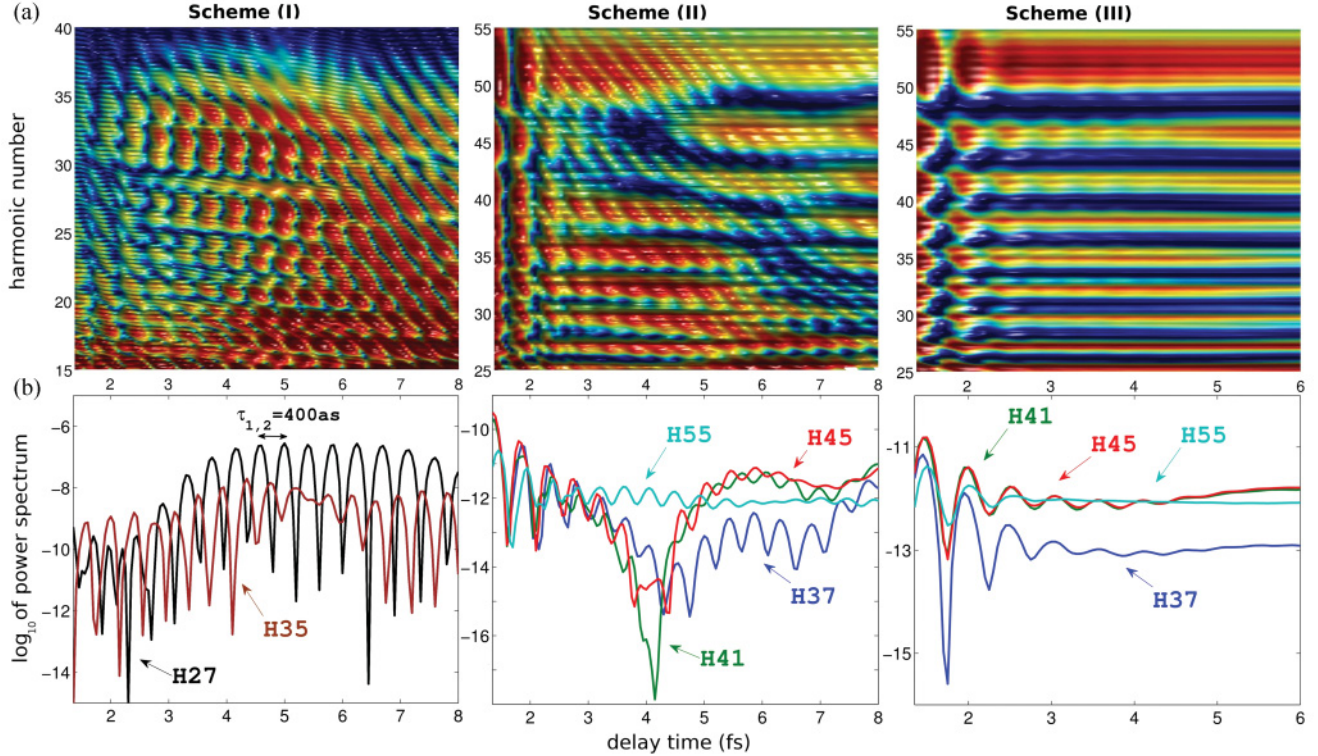
FIG. 2. (Color online) (a) Dependence of harmonic spectra on pump-probe delay time t_{del} for schemes I–III (see text and Table I). (b) Horizontal cuts through panel (a) for selected harmonics.

III the photon energy of the pump pulse to $\omega_{\text{pump}} = 0.28$ a.u. and decrease the pump intensity to $I_{\text{pump}} = 10^{11}$ W/cm^2. Very small populations appear now on the highest surface $\sigma_g 2p$ (see Table I), and the spectra shown in Fig. 2 (scheme III) show oscillations of a period equal to 430 as. Their amplitude decays rapidly at delays larger than 3 fs and no oscillations are seen at larger time delays, at which the nuclear wave packets on the two lower surfaces no longer overlap. Thus in scheme III we see indeed oscillation of MHOHG originating from pure coherent superposition of the two lower states, leading to similar decay of ionization oscillations as seen in Ref. [8]. In Ref. [11], the authors suggested that the delay-dependent minima of oscillations seen in MHOHG in their Figs. 1 and 3 occur at zeros of the electron dipole acceleration. In order to investigate in more detail this correlation related to such huge cancellations of the harmonic signal we calculate the time profile of harmonics using the Morlet-wavelet $W(t,\omega)$ transform of the acceleration $a(t)$, as defined via Eq. (2) in Ref. [16]. We set the width of the Gaussian time window to $\sigma\eta = 2\pi$ and our ω corresponds to $\xi = \frac{\eta}{s}$ defined in Ref. [16]. We plot in Fig. 3 $|W(t,\omega)|$ as a contour plot for two selected time delays $t_{\text{del}} = 5$ fs and $t_{\text{del}} = 5.2$ fs. In Fig. 3, $t = 0$ corresponds to the turn on of the probe pulse. We clearly see in Fig. 3 the ridges related to the two returning classical trajectories, and we observe a significant cancellation of a broad range of returning trajectories in Fig. 3(a) for the time delay $t_{\text{del}} = 5.2$ fs. We also plot on the right-hand side of Fig. 3, for the two selected time delays t_{del}, the average electron velocity of the bound electron v_B in the field-free (no probe pulse) evolution of the coherent superposition prepared by the

pump-pulse, i.e., we calculate $v_B(t) = \langle\psi_B(t)|\hat{p}_z/m_{\text{el}}|\psi_B(t)\rangle$, where ψ_B is calculated using Eq. (1) with the probe pulse turned off and $\hat{p}_z$ is the electron momentum operator. Note that the most suppressed trajectories (returning around the 1.4 optical cycle) originate from the tunneling occurring at the $t = 0.8$ cycle when the probe electric field is positive, and thus the electron born in the continuum acquires first a negative velocity, for $E(t) > 0$, and is next returning to the core with a positive velocity. As the two arrows indicate, considerable suppression of harmonic emission occurs at times when the returning (continuum) electron and bound electron have opposite average velocities, i.e., when the bound and recollision electron counterpropagate. A similar effect was also observed in Refs. [4,5] where the asymmetry of photoelectrons was directly correlated to the direction of the average velocity of the bound electron.

In summary, we have performed exact non-Born-Oppenheimer simulations of MHOHG by a coherent superposition of three electronic states: an initial bound state ($\sigma_g 1s$) and two dissociative states ($\sigma_u 1s$ and $\sigma_g 2p$) in T$_2^+$. Three population schemes are explored and proposed to illustrate extreme sensitivity of the MHOHG spectra to the time delay t_{del} between the ultrashort pump pulse for preparation of the CEWPs and the probe ionizing pulse for MHOHG. Thus in schemes I and II as illustrated in Fig. 2, extreme oscillations in the MHOHG spectra are obtained as a function of t_{del} due to non-negligible populations of the second excited state $\sigma_g 2p$. In scheme I, an oscillatory intensity pattern with a period $\tau_{2,3} \approx 400$ as is shown to correspond to the coherent oscillatory motion of electron density due to in-phase and out-of-phase
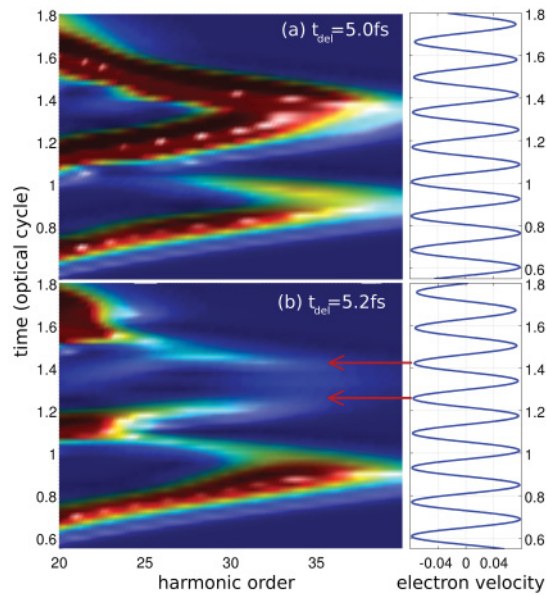
FIG. 3. (Color online) Time frequency spectra (left) for scheme I for two pump-probe time delays $t_{\text{del}} = 5.0$ fs (a) and $t_{\text{del}} = 5.2$ fs (b) and free time evolution (no probe pulse) of electron velocity (right) following excitation by the pump pulse corresponding to scheme I.

combinations of $\sigma_u 1s$ and $\sigma_g 2p$ molecular orbitals on the corresponding two nearly parallel surfaces. Oscillatory motion of electron density on an attosecond time scale in CEWPs has been previously shown to be measurable from attosecond oscillatory asymmetric photoionization of CEWPs [4,5]. For the present work, we have investigated the interferences of a total harmonic signal from the coherent sum of two or more amplitudes of returning and recombining electrons ionized from different electronic states with energies $E_1(R)$, $E_2(R)$, and $E_3(R)$. In schemes I and II, as predicted in Ref. [10]

in the SFA model for atoms, a two-state interference is expected via the term $\cos[\omega_{23} t_{\text{del}} + \phi(\omega)]$ as a function of delay time t_{del}, thus corresponding to a change in the birth t_0 and recombination times t_c. For each fixed photon energy, there exist two possible electron trajectories characterized by fixed tunneling and recollision times t_0 and t_c, respectively. In the case of a coherent superposition of two electronic states of energies E_1 and E_2 the electron can tunnel at t_0 from the two different electronic states with the well-defined phases $-E_1 t_0/\hbar$ and $-E_2 t_0/\hbar$, respectively. Varying the probe-pump delay time t_{del} shifts the tunneling time t_0 and the recombination time t_c, resulting in a modulation of MHOHG signals by an interference term $\cos(\omega_{12} t_{\text{del}} + \phi)$. For scheme III where only significant populations occur in state 1 ($\sigma_g 1s$) and 2 ($\sigma_u 1s$), corresponding to electron transfer between protons in the CEWPs, the MHOHG spectra oscillations become weak with time delay t_{del} due to the rapid decrease of overlap between the initial $\nu = 0$ nuclear wave function in the $\sigma_g 1s$ state and the dissociative nuclear wave function in the $\sigma_u 1s$ electronic state as previously reported in the corresponding attosecond photoionization [4,5,8]. Clearly, high sensitivity of MHOHG spectra from CEWPs occurs for pump-probe delays t_{del}, which preserve nuclear overlap between different electronic states. Finally, using the semiclassical three-step model of MHOHG [2,3,7] which allows one to predict the direction of velocity of returning electron trajectories, it was possible to correlate extreme destructive interference in oscillatory MHOHG spectra due to opposite electron velocities of the CEWPS and the recombining electron wave packet (Fig. 3).

[1] A. D. Bandrauk and M. Y. Ivanov (Eds.) *Quantum Dynamic Imaging* (Springer, New York, 2011).

[2] F. Krausz and M. Ivanov, Rev. Mod. Phys. **81**, 163 (2009).

[3] P. B. Corkum and F. Krausz, Nat. Phys. **3**, 361 (2007).

[4] A. D. Bandrauk, S. Chelkowski, and H. S. Nguyen, Int. J. Quantum Chem. **100**, 834 (2004).

[5] S. Chelkowski, G. L. Yudin, and A. Bandrauk, J. Phys. B **39**, S409 (2006), and references therein.

[6] A. D. Bandrauk, S. Chelkowski, S. Kawai, and H. Lu, Phys. Rev. Lett. **101**, 153901 (2008).

[7] P. B. Corkum, Phys. Rev. Lett. **71**, 1994 (1993).

[8] A. D. Bandrauk, S. Chelkowski, P. B. Corkum, J. Manz, and G. L. Yudin, J. Phys. B **42**, 134001 (2009).

[9] J. P. Paz, S. Habib, and W. H. Zurek, Phys. Rev. D **47**, 488 (1993).

[10] D. B. Milosevic, J. Opt. Soc. Am. B **23**, 308 (2006).

[11] H. Niikura, D. M. Villeneuve, and P. B. Corkum, Phys. Rev. Lett. **94**, 083003 (2005).

[12] A. D. Bandrauk and S. Barmaki, Chem. Phys. **350**, 175 (2008); J. Mod. Opt. **54**, 1047 (2007).

[13] H. J. Wörner *et al.* Nature (London) **466**, 604 (2010); H. J. Wörner, J. B. Bertrand, P. B. Corkum, and D. M. Villeneuve, Phys. Rev. Lett. **105**, 103002 (2010).

[14] H.-C. Shao and A. F. Starace, Phys. Rev. Lett. **105**, 263201 (2010).

[15] Armelle de Bohan, P. Antoine, D. B. Milosevic, and B. Piraux, Phys. Rev. Lett. **81**, 1837 (1998).

[16] C. W. Chandre and T. Uzer, Physica D **181**, 171 (2003).